

Dimension of Time in Strange Attractors

Robert J. Krawczyk
College of Architecture, Illinois Institute of Technology
3360 South State Street, Chicago, IL 60616, USA
krawczyk@iit.edu

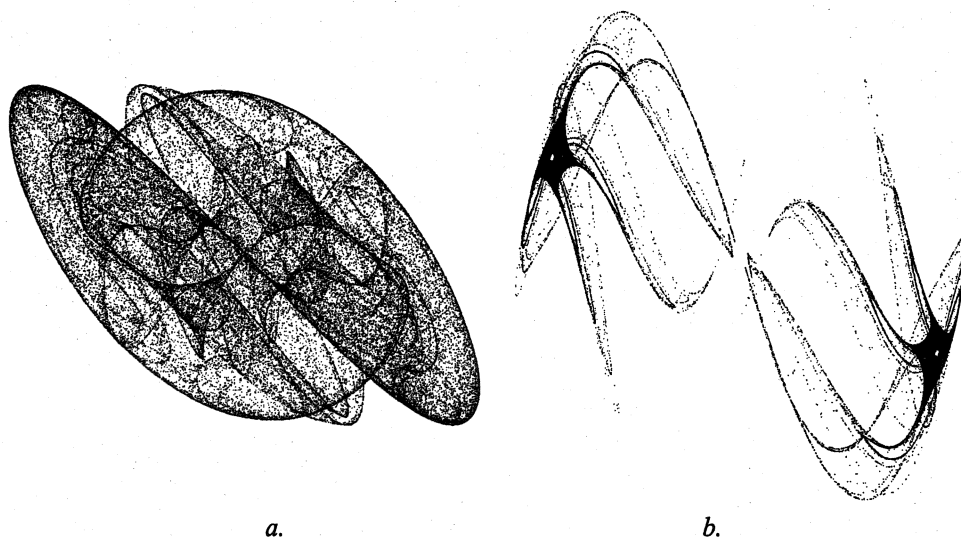
Abstract

In the rendering of strange attractors a number of methods are outlined how the element of time can be used. Time can be represented as the number of times a mapped location is selected or when the location is selected. A variety of coloring schemes based on the concept of time are also discussed. The other aspect time serves is the ability to visually suggest three-dimensional surfaces within two-dimensional strange attractors. This last effect enables strange attractors to be artistically presented in a manner that adds dynamic properties and ghostly interiors to static images. The added third dimension suggests surfaces that visually want to be logically followed but can never be.

1. Introduction

Clifford Pickover [1] extended some of his previous writings on three-dimensional chaotic or strange attractors [2,3] by including a series of two-dimensional attractors based on a simple equation consisting of sine functions. What was intriguing about these images was the variations possible by the execution of a simple iterative mapping with minor changes in parameters. The visual complexity of detail within the image and the visual perception of a third-dimension as the curves began to suggest surfaces became the starting point for development. Figure 1 displays two such attractors based on Equation 1 [4].

$$\begin{aligned}x_{t+1} &= \sin(by_t) + c \sin(bx_t) \\ y_{t+1} &= \sin(ax_t) + d \sin(ay_t)\end{aligned}\tag{Equation 1}$$



a. **Figure 1:** *Pickover's strange attractors* *b.*

This single equation generated one image in which the mapped points begin to uncover a ghostly interior, while a second set of parameters generated two separate areas of attraction from which curving lines emulate. Pickover includes another eight images based on the same equation and a few others based on variations to Equation 1. The symmetry exhibited in these images can also be found in other equations he developed. Pickover [2,3] also discusses rendering issues of three-dimensional attractors. Some of these methods of shading and representing time are again included [1] but in more detail.

Based on the work of Pickover and the same method of rendering, Joel [5] suggested other similar equations and transformations, such as, rotation, mirroring, and scaling. A very extensive study of attractors was performed by Sprott [6]. He covers the basics of computing attractors, a dictionary of possible equations and parameters, and the study of thousands, if not millions, of attractors. He includes one, two, three, and four-dimensional attractors, as well as, a number of methods of visualizing them, such as, shadows, coloring schemes, stereo pairs, slicing, and projections.

2. Time and Density

Pickover [1] noted that an attractor could result in three possible cases: it will converge to a fixed point, it will enter into a repeating succession of values, or it will exhibit chaos and gradually fill some complex region. Paul Bourke demonstrates this by creating a set of what he calls "swirling tendrils" [7]. He uses Equation 2 to generate a series of images. This equation he which attributes to Dewdney [8] is a variation of the ones that Pickover developed. In reproducing these images, a time limit of 100,000 computations was used. This single attractor displays some interesting visual aspects depending on the values selected, Figure 2 [9].

$$\begin{aligned} x_{t+1} &= \sin(ay_t) - \cos(bx_t) \\ y_{t+1} &= \sin(cx_t) - \cos(dy_t) \end{aligned} \quad (\text{Equation 2})$$

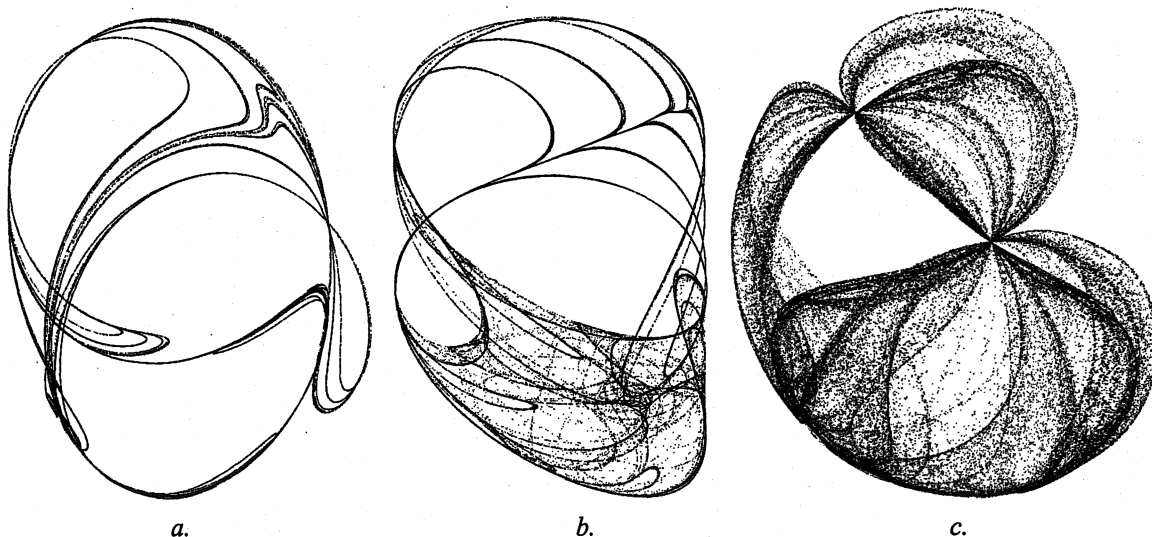


Figure 2: Bourke's swirling tendrils

In the first, all the points lie on curves with little or no deviation. In the second, a distinct curve is also traced but you can begin to see lighter trails forming. In the third, the distribution of points is much greater and because of the density of points in certain areas, surfaces begin to appear. The curves which are a greater congregation of points begin to represent the edges of these surfaces. A third dimension is

only implied by these visual cues since the equations are a two-dimensional mapping. In this case density of points is controlled by time or time can be seen to begin to give two-dimensional attractors a three-dimensional visual appearance. The distance between the points controls apparent shading.

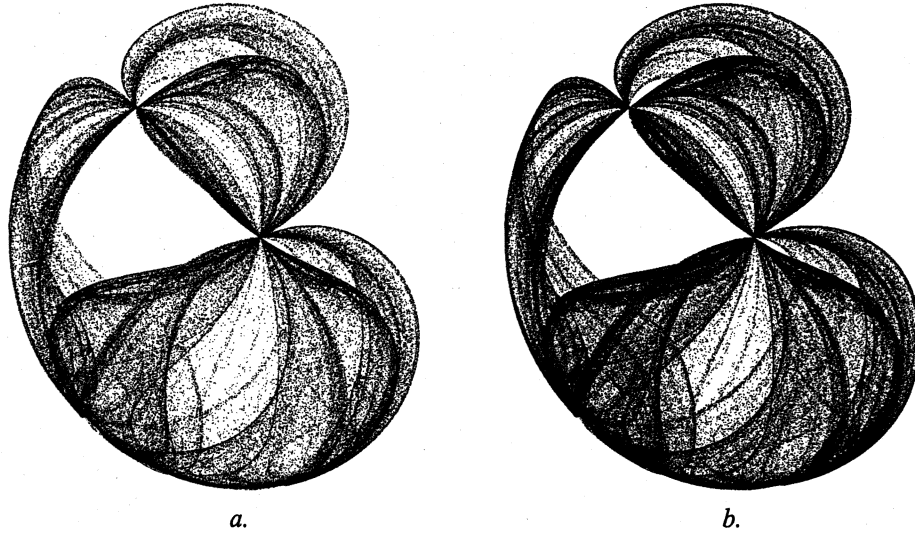


Figure 3: Comparison of density.

When time is increased, the density of the points further draws out either hidden areas within regions of the attractor or it strengthens what appears to be edges of three-dimensional surfaces. Figure 3a. displays the Bourke's third attractor using 200,000 points. Since an increase of time will generate finer detail at a given image resolution, rather than just increasing the time element, a percent fill approach was developed. In Figure 3b. the computation of the attractor was terminated when 30% of the potential image points were selected. This percent fill approach seems to be an improved method to generate consistent attractors at any image resolution, since predicting the time, number of points to compute, is impossible.

The attractor in Figure 3b. required 630,276 point computations to fill 30% of an 780x780 pixel image. The chart in Figure 4 displays the point computations required to fill 5,776 empty pixels for each percent. The last percent required over 53,000 computations.

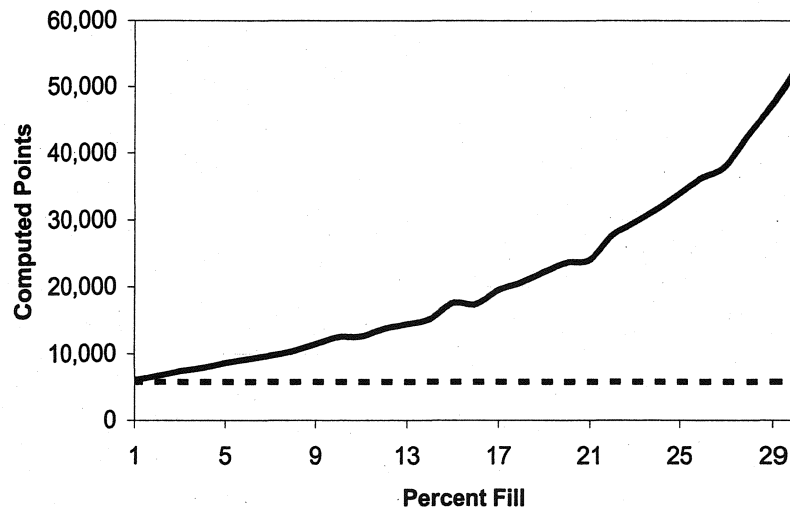


Figure 4: Number of computed points per percent.

The chart also begins to display the number of points that are repeated in the computations. In comparison, the two previous images of 100,000 and 200,000 computations had a percent fill 10.8% and 17.0%. All of these images rely on density for shading since only a single color is used, black.

3. Time and Points

Instead of density or a single color, representing the points within an attractor, Pickover [1] suggests that when points are computed the total number of times a point or pixel is selected become the criteria for assigning a color to it. Continuing with the attractor from Bourke, Figure 5a. displays the attractor based on 100,000 computations with the number of times each location was selected or hit recorded. The results were then normalized to 256 levels and then an equalize filter applied. As an alternative method, Figure 5b. the last time a location was selected is recorded instead. Then the results were normalized to 256 levels, the equalize filter was not applied. A close visual inspection indicates a wider range of grayscale values in the second method than the first. Pickover notes that the first method requires an extremely large number of computations to be able to distribute the number of hits at any meaningful level.

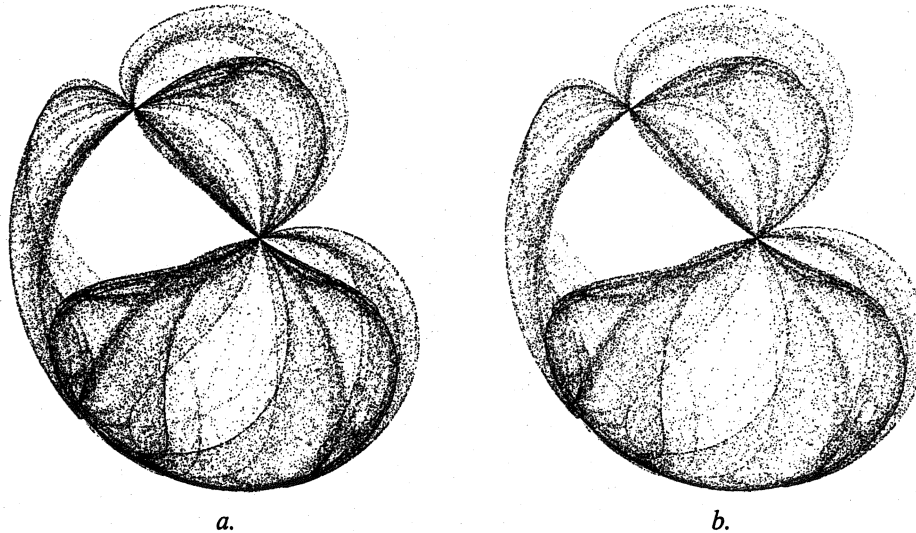


Figure 5: Comparing number of hits with when hit.

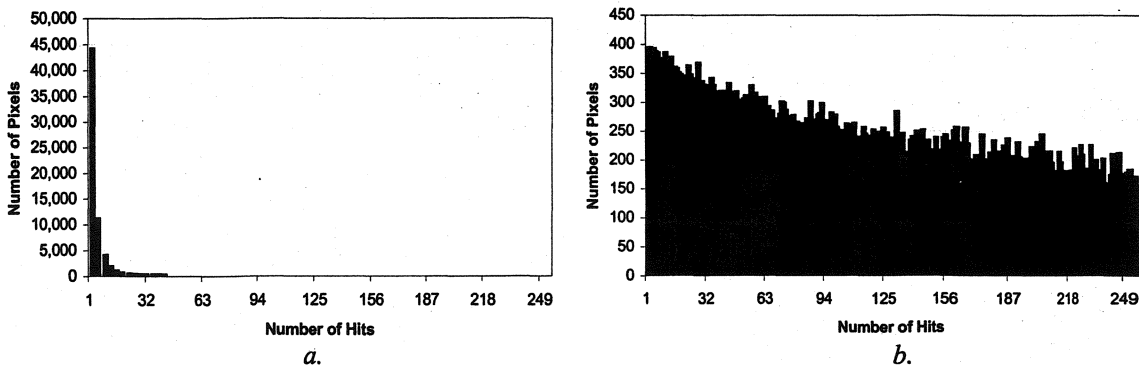


Figure 6: Number of computing points per percent.

To better see this difference, a graph of the grayscale values was developed for each method. Figure 6a. show the distribution based on the number of hits and 6b. the distribution based on the last hit. When

these graphs are summarized, as in Figure 7a., it is clear that the distribution is finer by the last hit method. When the image is equalized, the grayscale is readjusted but still not redistributed at a finer level. Additional grayscale values are not produced, they are just moved. The more grayscale values that can be generated, the better the detail of the attractor will be exposed, and the appearance of surfaces and edges become more profound. This is the goal of rendering the attractor. A good discussion of the problems with the equalization method can be found in Oliver et al [10].

Color	Points: 100,000		Points: 30%	
0 to 64	62,486	21,226	173,259	85,617
65 to 128	17	16,207	19	41,264
129 to 192	1	13,672	1	27,096
193 to 255	1	11,400	1	19,303
Total:	62,505	62,505	173,280	173,280
	By hits	By last hit	By hits	By last hit

Figure 7: Summary of the grayscale distribution.

To further explore this distribution, the attractors were generated a second time using a 30% fill criteria. The results are displayed in Figure 8. The grayscale values are summarized in Figure 7b. The same type of distribution as before is exhibited. Figure 8b. demonstrates the distribution by last hit, it develops much larger areas of softer levels of grays. To further enhance these levels, a very light gaussian blur can be applied to the final image.

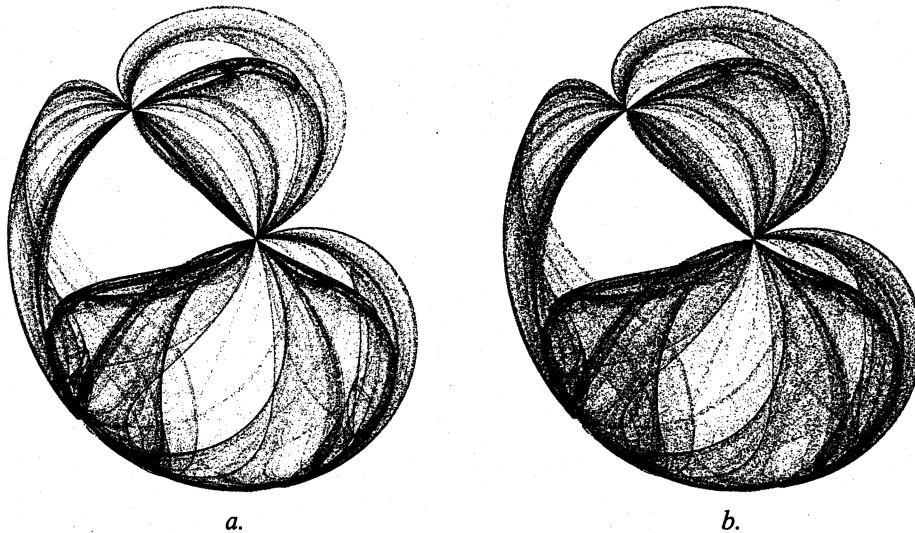


Figure 8: Final renderings by number of hits and by last hit.

4. Expanding Time

Figure 9a. displays another Bourke attractor based on Equation 2 [11]. This particular attractor is one that generates a large number of repeating values so that distinct curves are created with a small number of points appearing between the curves. Computing more points, adding time, will not introduce any in-between points. Devaney [12] discussed a random iteration algorithm for iterated function systems that seemed appropriate for expanding the generated curves. This method is based on the random selection from a range of specific values. For these attractor this basic concept was used in two variations. The

first, Figure 9b. used a percent offset to compute related attractors. From these computed values any one was selected. The result is a soft haze surrounding each of the curves in the attractor. The second, Figure 9c. used the same percent offset, but the possible random values were selected from a fixed interval. The haze surrounding the curves was greater in area. In both cases, the region between the curves begins to be filled and create possible surfaces.

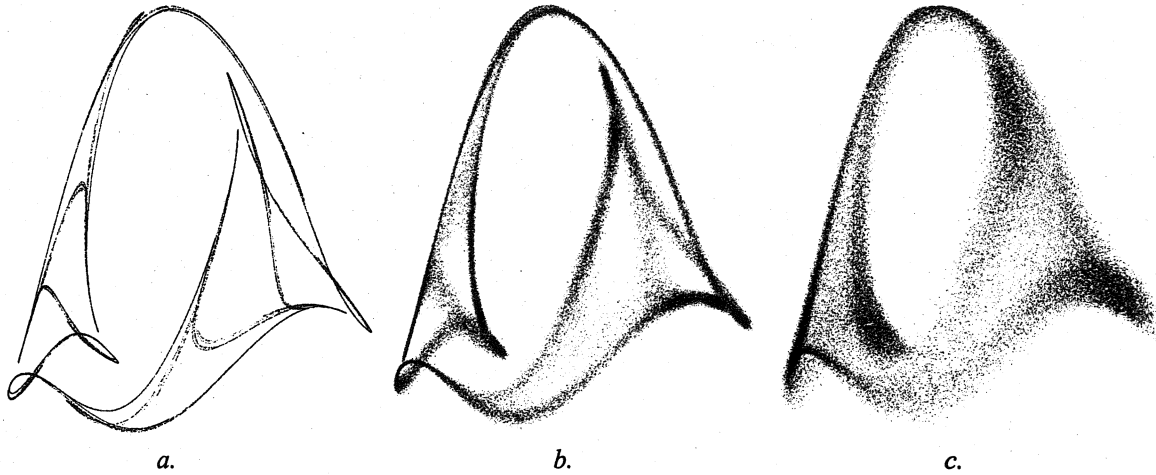


Figure 9: *Random selection of values for an attractor.*

While selecting values for a variety of attractors, it was noticed that related images were created when a single parameter was modified. For example, the attractor based on Equation 3 can generate an series having an unraveling motion when only the first parameter is changed [13]. A series such as this can be viewed as static images, frozen time, or animated to give an attractor the added dimension of motion. Other attractors were found that developed an unfolding motion. The challenge is to determine in a specific attractor which parameter or parameters can be changed and their range to generate this effect. It does offer an unique display of a related family of attractors.

$$\begin{aligned} x_{t+1} &= |\sin^3(ay_t)| + \cos(bx_t) \\ y_{t+1} &= |\sin^2(cx_t)| - \cos^2(dy_t) \end{aligned} \quad \text{(Equation 3)}$$

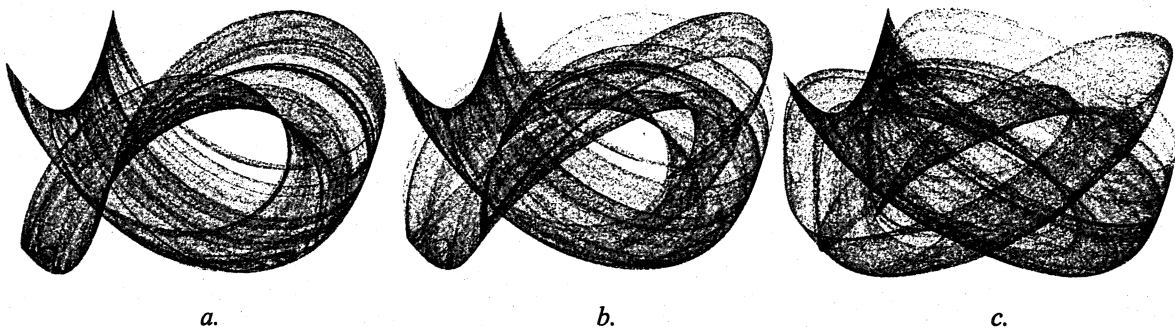


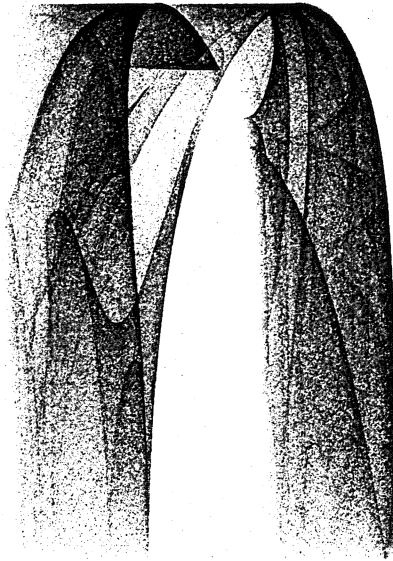
Figure 10: *Unraveling an attractor.*

5. Dimension of Time

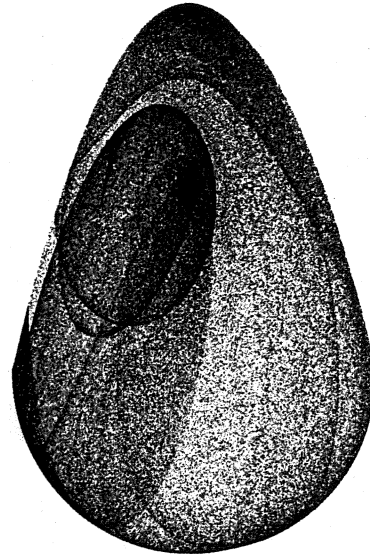
Joel [5] noted in his images of attractors the qualities of wisps of smoke being blown by a gentle wind, ropes coiling in space, and small beads strung along an invisible wire. Bourke titled his attractors swirling tendrils, a term related the botany. He also commented on the visualization of three dimensions

in two-dimensional attractors [14], many of the examples are more tendril like, while a few exhibit major surfaces.

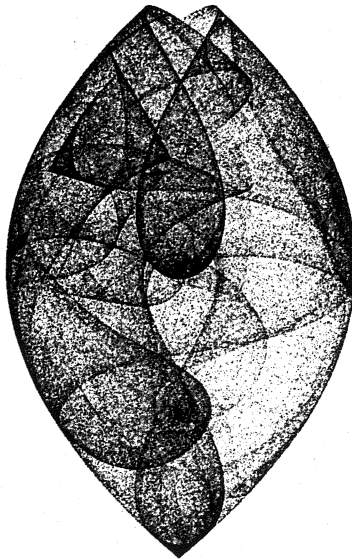
Figures 11 and 12 display a sample from the current series of rendered attractors based on this concept of dimension of time. Similar to previous comments, the relationship of the image of the attractors to nature was apparent. Many of these could have been inspired from natural forces, such as, wind and water, or earthen formations. For example, the stone series explores the possible subsurface patterns in nature that are not visible to us; the smoldering images smoke, others; folding, bending, twisting, draping and crumpling of identifiable materials or organisms. The third dimension is determined by the perception of the viewer coupled with the created intent by selection of attractor and its parameters. The forms include a ghostly view into an imaginary core. The swirling patterns gently display possible subsurface structures that cannot be logically followed through any dimension. Dimensions become ambiguous as your perception attempts to combine the individual points so they complete a whole, one that is devoid of context.



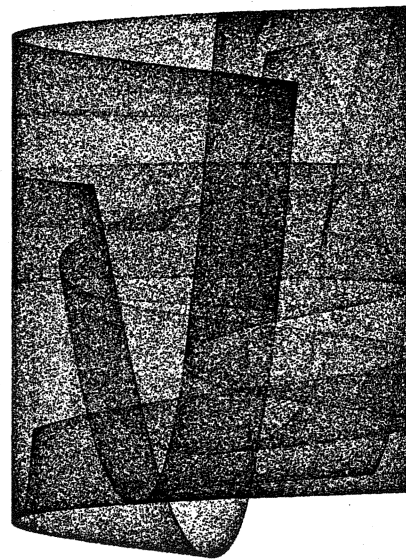
Draping Fall II, 2002



Touched Stone III, 2002

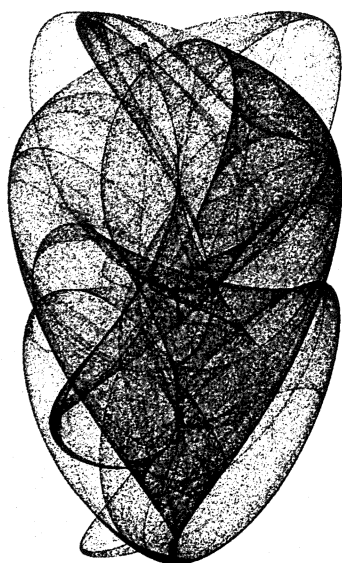


Within Stone I, 2002



Folds Over I, 2002

Figure 11: *Examples of completed strange attractors.*



Ringing Wave I, 2002



Smoldering Rise I, 2002

Figure 12: Examples of completed strange attractors.

For this paper the attractors were rendered grayscale on a white background. The actual images are colored in 256 levels of red on a solid black background and rendered to a resolution of about 5,000 x 5,000 pixels. The number of point computations required for these ranges from 12-to-59 million points. The current series can be viewed at: www.netcom.com/~bitart

References

- [1] C. Pickover, *Chaos in Wonderland*, St. Martin's Press, New York, pp. 11-13, 55-58, 75-77, 86-87, 209, 210, 213, 1994.
- [2] C. Pickover, A note on rendering 3-D strange attractors, *Computers & Graphics*, Vol. 12, No. 2, pp. 263-267, 1988
- [3] C. Pickover, *Computers and the Imagination*, St. Martin's Press, New York, pp. 285-286. 1991.
- [4] Figure 1, Equation 1 (a, b, c, d): $a = (-2.90, -2.03, 1.44, 0.70)$; $b = (-2.16, -0.64, 1.2, 1.00)$.
- [5] W. Joel, A Simple Attraction, *Computers & Graphics*, Vol. 16, No. 1, pp. 41-43, 1992.
- [6] J. Sprott, *Strange Attractors, Creating Patterns in Chaos*, M&T Press, New York, 1993.
- [7] P. Bourke, Swirls, *The Pattern Book: fractals, art, and nature*, edited by C. Pickover, World Scientific Publishing, Singapore, pp. 197-198. 1995.
- [8] A. Dewdney, Probing the strange attractions of chaos, *Scientific American*, pp. 108-111. July, 1987.
- [9] Figure 2 Equation 2 (a, b, c, d): $a = (-2.24, 0.43, -0.65, -2.43)$; $b = (-2.70, -0.08, -0.86, -2.20)$; $c = (-2.00, -1.00, -1.00, -1.50)$.
- [10] D. Oliver et al, *PC Graphics Unleashed*, Sams Publishing, Indianapolis, pp. 115-128, 1994.
- [11] Figure 9 Equation 2 (a, b, c, d); $a = (0.44, -1.22, 2.50, -1.50)$.
- [12] R. Devaney, *Chaos and Fractals, The Mathematics Behind the Computer Graphics*, American Mathematical Society, Providence, p. 141. 1989.
- [13] Figure 10 Equation 3 (a, b, c, d): $a = (-5.0, -0.5, -1.1, 7.5)$; $b = (-5.25, -0.5, -1.1, 7.5)$; $c = (-6.0, -0.5, -1.1, 7.5)$
- [14] P. Bourke, Random Attractors Found Using Lyapunov Exponents, website URL is <http://astronomy.swin.wdu.au/~pbourke/fractals/lyapunov>, October, 2001.